Mechanics and Mechanical Engineering
Vol. 20, No. 3 (2016) 209–231

Dispresion Analysis in a Fluid–Filled and Immersed Transversely Isotropic Thermo–Electro–Elastic Hollow Cylinder

R. Selvamani
Department of Mechanical Mathematics
Karunya University, Coimbatore
TamilNadu, India
selvam1729@gmail.com

Received (22 January 2016)
Revised (16 February 2016)
Accepted (24 March 2016)

The dispersion analysis in a fluid filled and immersed thermo–electro elastic hollow cylinder composed of homogeneous, transversely isotropic material is studied within the frame work of linear theory of elasticity. The motions of the cylinder are formulated using the constitutive equations of a transversely isotropic piezo–thermo elastic material with a preferred material direction collinear with the longitudinal axis of the cylinder. The equations of motion of the internal and external fluids are formulated using the constitutive equations of an inviscid fluid. Displacement potentials are used to solve the equations of motion of the hollow cylinder and the fluids. The perfect–slip boundary condition is employed at the fluid–solid interface to find the frequency equation of the coupled system consisting of the cylinder, internal and external fluid. The non–dimensional frequencies obtained by the author are compared with the result of Paul and Raju [Paul, H. S., Raju, D. P, Asymptotic analysis of the modes of wave propagation in a piezoelectric solid cylinder. J. Acoust. Soc. Am. 71(2)(1982) 255–263] which matches well and shows the exactness of the author's method. The computed dimensionless frequency, phase velocity, attenuation, thermo mechanical coupling factor and specific loss are plotted in the form of dispersion curves for the material PZT-5A.

Keywords: wave propagation in piezoelectric cylinder/plates, solid–fluid interaction, thermal cylinders/plates, mechanical vibrations, cylinder immersed in fluid, Bessel/Hankel functions, sensors/actuators.

1. Introduction

Piezoelectric materials have been used extensively in the construction of sensors and transducers due to their direct and converse piezoelectricity effects. The direct piezoelectric effect is used in sensing applications, such as in force or displacement sensors. The converse piezoelectric effects are used in transduction applications, such as in motors and device that precisely control positioning, and in generating sonic and ultra sonic signals. The piezoelectric materials are physically strong and

chemically inert, and they are relatively inexpensive to manufacture. The composition, shape and dimension of piezoelectric ceramic elements can be tailored to meet the requirements of a specific purpose. Ceramics manufactured from formulations of lead zirconate / lead titanate exhibit greater sensitivity and higher operating temperatures, relative to ceramics of other compositions and the materials PZT-5A are most widely used piezoelectric ceramics.

Early studies in elastic wave propagation in cylindrical waveguides are mostly concerned with isotropic cylinders. The historical development of the problem has been given by Meeker and Meitzler [1].Two–part study by Mirsky [2] was devoted to the problem of longitudinal waves propagation in transversely isotropic circular cylinders using an approach based on potential functions.The propagation of compressional elastic waves along an anisotropic circular cylinder with hexagonal symmetry was first studied by Morse [3].

Theoretical studies on electroelastic wave propagation in anisotropic piezoceramic cylinders have also been pursued for many years. The approach usually applied for piezoelectric solids is the simplification of Maxwell's equations by neglecting magnetic effects, conduction, free charges, and displacement currents. Studies by Tiersten [4]should be mentioned among the early notable contributions to the topic of the mechanics of piezoelectric solids. Electro elastic governing equations of piezoelectric materials are presented by Parton and Kudryavtsev [5]. Shul'ga [6] studied the propagation of axisymmetric and non–axisymmetric waves in anisotropic piezoceramic cylinders with various prepolarization directions and boundary conditions.

Rajapakse and Shou [7] solved the coupled electroelastic equations for a long piezoceramic cylinder by applying Fourier integral transforms. Paper by Wang [8] should be mentioned among the studies of cylindrical shells with a piezoelectric coat. Ebenezer and Ramesh [9] analyzed axially polarized piezoelectric cylinders with arbitrary boundary conditions on the flat surfaces using the Bessel series. Berg et al. [10] assumed electric field not to be constant over the thickness of piezoceramic cylindrical shells. Later, Botta and Cerri [11] extended this approach and compared their results with those in which the effect of variable electric potential was not considered. Kim and Lee [12] studied piezoelectric cylindrical transducers with radial polarization and compared their results with those obtained experimentally and numerically by the finite element method.

The coupling between the thermal/electric/elastic fields in piezo electric materials provides a mechanism for sensing thermo mechanical disturbances from measurements of induced electric potentials, and for altering structural responses via applied electric fields. One of the applications of the piezo-thermoelastic material is to detect the responses of a structure by measuring the electric charge, sensing or to reduce excessive responses by applying additional electric forces or thermal forces actuating. If sensing and actuating can be integrated smartly, a so–called intelligent structure can be designed. The coupling between the thermo-elastic and pyro–electric effects is important to qualify the effect of heat dissipation on the propagation of wave at low and high frequencies.

The thermo- piezoelectric theory was first proposed by Mindlin [13], later he derived the governing equations of a thermo–piezoelectric plate [14]. The physical laws for the thermo–piezoelectric materials have been discussed by Nowacki [15, 16]. Chandrasekhariah [17, 18] presented the generalized theory of thermo–

piezoelectricity by taking into account the finite speed of propagation of thermal disturbance. Yang and Batra [19] studied the effect of heat conduction on shift in the frequencies of a freely vibrating linear piezoelectric body with the help of perturbation methods. Sharma and Pal [20] discussed the propagation of Lamb waves in a transversely isotropic piezothermoelastic plate. Sharma et al [21]investigated the free vibration analysis of a homogeneous, transversely isotropic, piezothermoelastic cylindrical panel based on three dimensional piezoelectric thermoelasticity. Ponnusamy [22] studied the wave propagation in generalized thermo-elastic cylinder of arbitrary cross section using Fourier collocation method.Dispersion analysis of generalized magneto-thermoelastic waves in a transversely isotropic cylindrical panel is analyzed by Ponnusamy and Selvamani [23].

Sinha et al [24] have studied the axisymmetric wave propagation in circular cylindrical shell immersed in a fluid, in two parts. In Part I, the theoretical analysis of the propagation modes is discussed and in Part II, the axisymmetric modes excluding tensional modes are obtained theoretically and experimentally and are compared. Berliner and Solecki [25] have studied the wave propagation in a fluid loaded transversely isotropic cylinder. In that paper, Part I consists of the analytical formulation of the frequency equation of the coupled system consisting of the cylinder with inner and outer fluid and Part II gives the numerical results.

Selvamani and Ponnusamy [26] studied the wave propagation in a generalized thermo elastic plate immersed in fluid. Recently, the dynamic response of a solid bar of cardioidal cross–sections immersed in an inviscid fluid was performed by Selvamani and Ponnusamy [27]. Dayal [28] investigated the free vibrations of a fluid loaded transversely isotropic rod based on uncoupling the radial and axial wave equations by introducing scalar and vector potentials. Nagy [29] studied the propagation of longitudinal guided waves in fluid–loaded transversely isotropic rod based on the superposition of partial waves.

The present article emphasis the dispersion analysis in a fluid filled thermo–piezo elastic hollow cylinder immersed in an inviscid fluid. The frequency equations are obtained from the solid–fluid interfacial boundary conditions. The computed dimensionless frequency, phase velocity, attenuation, thermo mechanical coupling factor and specific loss are plotted in the form of dispersion curves for the material PZT-5A.To discuss the accuracy of the author's result with the existing literature, the frequency equations are first solved by omitting the fluid medium and thermo coupling and the dimensionless eigen frequencies are obtained. The frequencies are compared with the frequencies obtained by Paul and Raju [30] for longitudinal mode, and it is noted that all in agreement with the author's result as shown in Tab. 1.

2. Formulation of the problem

The system under consideration is shown in Fig. 1. It consists of an infinitely long linearly elastic homogeneous transversely isotropic piezo–thermo elastic cylinder with inner radius $a$and outer radius bThe cylinder is filled with an irrotational, inviscid fluid with density ρ_1^f and an acoustic phase velocityc_1. The cylinder is also immersed in a second irrotational, inviscid fluid with density ρ_2^f.

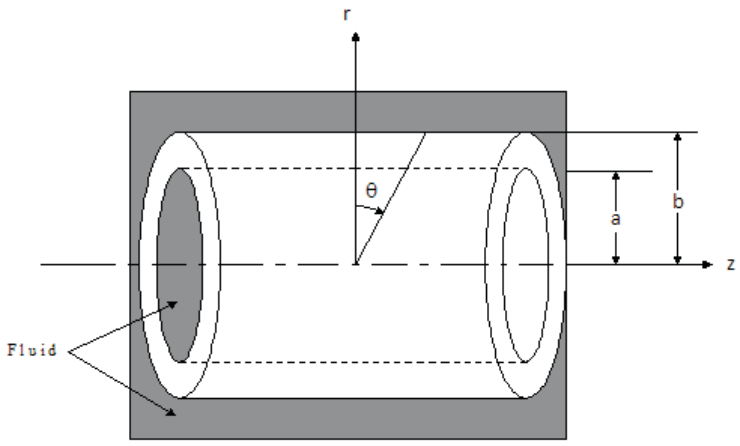

Figure 1 The fluid–filled hollow cylinder immersed in an infinite fluid

Since the system is assumed to be linear, so that the linearized three–dimensional stress equations of motion can be used for both the cylinder and fluid. The complete equations governing the behavior of piezoelectric cylinder have been considered from Paul [31]. In cylindrical coordinates(r, θ, z), the equations of motion in the absence of body force are:

$$\begin{aligned}
&\sigma_{rr,r} + r^{-1}\sigma_{r\theta,\theta} + \sigma_{rz,z} + r^{-1}\left(\sigma_{rr} - \sigma_{\theta\theta}\right) = \rho u_{r,tt} \\
&\sigma_{r\theta,r} + r^{-1}\sigma_{\theta\theta,\theta} + \sigma_{\theta z,z} + 2r^{-1}\sigma_{r\theta} = \rho u_{\theta,tt} \\
&\sigma_{rz,r} + r^{-1}\sigma_{\theta z,\theta} + \sigma_{zz,z} + r^{-1}\sigma_{rz} = \rho u_{z,tt}
\end{aligned} \tag{1}$$

The heat conduction equation for transversely isotropic medium is

$$\begin{aligned}
&K_1\left(T_{,rr} + r^{-1}T_{,r} + r^{-2}T_{,\theta\theta}\right) + K_3 T_{,zz} - \rho c_v T_{,t} = T_o\left(\beta_1\left(e_{rr} + e_{\theta\theta}\right)\right. \\
&\left.+\beta_3 e_{zz} - p_3\phi_{,z}\right)_{,t}
\end{aligned} \tag{2}$$

The electro static equation which satisfies the Gaussian equation is

$$\frac{1}{r}\frac{\partial}{\partial r}\left(rD_r\right) + \frac{1}{r}\frac{\partial D_\theta}{\partial \theta} + \frac{\partial D_z}{\partial r} = 0 \tag{3}$$

The elastic, the piezoelectric and dielectric matrices of the 6mm crystal class, the piezoelectric relations are:

$$\begin{aligned}
\sigma_{rr} &= c_{11}e_{rr} + c_{12}e_{\theta\theta} + c_{13}e_{zz} - \beta_1 T - e_{31}E_z \\
\sigma_{\theta\theta} &= c_{12}e_{rr} + c_{11}e_{\theta\theta} + c_{13}e_{zz} - \beta_1 T - e_{31}E_z \\
\sigma_{zz} &= c_{13}e_{rr} + c_{13}e_{\theta\theta} + c_{33}e_{zz} - \beta_3 T - e_{33}E_z \\
\sigma_{r\theta} &= c_{66}e_{r\theta} \\
\sigma_{\theta z} &= c_{44}e_{\theta z} - r^{-1}e_{15}E_\theta \\
\sigma_{rz} &= 2c_{44}e_{rz} - e_{15}E_r \\
D_r &= e_{15}e_{rz} + \varepsilon_{11}E_r \\
D_\theta &= e_{15}e_{\theta z} + r^{-1}\varepsilon_{11}E_\theta \\
D_z &= e_{31}\left(e_{rr} + e_{\theta\theta}\right) + e_{33}e_{zz} + \varepsilon_{33}E_z + p_3 T
\end{aligned} \tag{4}$$

where σ_{rr}, $\sigma_{\theta\theta}$, σ_{zz}, $\sigma_{r\theta}$, $\sigma_{\theta z}$, σ_{rz} are the stress components, e_{rr}, $e_{\theta\theta}$, e_{zz}, $e_{r\theta}$, $e_{\theta z}$, e_{rz} are the strain components, T is the temperature change about the equilibrium temperature T_o, c_{11}, c_{12}, c_{13}, c_{33}, c_{44} and $c_{66} = (c_{11} - c_{12})/2$ are the five elastic constants, β_1, β_3 and K_1, K_3 respectively thermal expansion coefficients and thermal conductivities along and perpendicular to the symmetry, ρ is the mass density, c_v is the specific heat capacity, $p_3$is the pyroelectric effect.

The strain e_{ij} are related to the displacements are given by:

$$\begin{aligned}
&e_{rr} = u_{r,r} \quad e_{\theta\theta} = r^{-1}\left(u_r + u_{\theta,\theta}\right) \quad e_{zz} = u_{z,z} \\
&e_{r\theta} = u_{\theta,r} + r^{-1}\left(u_{r,\theta} - u_\theta\right) \quad e_{z\theta} = \left(u_{\theta,z} + r^{-1}u_{z,\theta}\right) \\
&e_{rz} = u_{z,r} + u_{r,z}
\end{aligned} \tag{5}$$

Substituting the Eqs. (4) and (5) in the Eqs. (1)–(3), results in the following three–dimensional equations of motion, heat and electric conductions as follows:

$$\begin{aligned}
&c_{11}\left(u_{rr,r} + r^{-1}u_{r,r} - r^{-2}u_r\right) - r^{-2}\left(c_{11} + c_{66}\right)u_{\theta,\theta} + r^{-2}c_{66}u_{r,\theta\theta} + c_{44}u_{r,zz} \\
&+ \left(c_{44} + c_{13}\right)u_{z,rz} + r^{-1}\left(c_{66} + c_{12}\right)u_{\theta,r\theta} + \left(e_{31} + e_{15}\right)V_{,rz} = \rho u_{r,tt} \\
&r^{-1}\left(c_{12} + c_{66}\right)u_{r,r\theta} + r^{-2}\left(c_{66} + c_{11}\right)u_{r,\theta} + c_{66}\left(u_{\theta,rr} + r^{-1}u_{\theta,r} - r^{-2}u_\theta\right) \\
&+ r^{-2}c_{11}u_{\theta,\theta\theta} + c_{44}u_{\theta,zz} + r^{-1}\left(c_{44} + c_{13}\right)u_{z,\theta z} + \left(e_{31} + e_{15}\right)V_{,\theta z} = \rho u_{\theta,tt} \\
&c_{44}\left(u_{z,rr} + r^{-1}u_{z,r} + r^{-2}u_{z,\theta\theta}\right) + r^{-1}\left(c_{44} + c_{13}\right)\left(u_{r,z} + u_{\theta,\theta z}\right) \\
&+ \left(c_{44} + c_{13}\right)u_{r,rz} + c_{33}u_{z,zz} + e_{33}V_{,zz} + e_{15}\left(V_{,rr} + r^{-1}V_{,r} + r^{-2}V_{,\theta\theta}\right) = \rho u_{z,tt} \\
&K_1\left(T_{,rr} + r^{-1}T_{,r} + r^{-2}T_{,\theta\theta}\right) + K_3 T_{,zz} - \rho c_v T_{,t} = T_o\left(\beta_1(u_{r,r} + r^{-1}u_{\theta,\theta}\right. \\
&\left. + r^{-1}u_r) + \beta_3 u_{z,z} - p_3\phi_{,z}\right)_{,t} \\
&e_{15}\left(u_{z,rr} + r^{-1}u_{z,r} + r^{-2}u_{z,\theta\theta}\right) + \left(e_{31} + e_{15}\right)\left(u_{r,zr} + r^{-1}u_{r,z} + r^{-1}u_{\theta,z\theta}\right) \\
&+ e_{33}u_{z,zz} - \varepsilon_{33}V_{,zz} - \varepsilon_{11}\left(V_{,rr} + r^{-1}V_{,r} + r^{-2}V_{,\theta\theta}\right) = 0
\end{aligned} \tag{6}$$

3. Boundary conditions

3.1. *Mechanical boundary conditions*

In the solid–fluid interface problems, the normal stress of the cylinder is equal to the negative of the pressure exerted by the fluid and the displacement component in the

normal direction of the lateral surface of the cylinder is equal to the displacement of the fluid in the same direction. These conditions are due to the continuity of the stresses and displacements of the solid and fluid boundaries. Since the fluid inviscid, it cannot sustain shear stress, the shear stress of the outer fluid is equal to zero.

$$\begin{aligned}[\sigma_{rr}, \sigma_{r\theta}, \sigma_{rz}, u_r] &= \left[-p_1^f, 0, 0, u_r^f\right], r = a \\ [\sigma_{rr}, \sigma_{r\theta}, \sigma_{rz}, u_r] &= \left[-p_2^f, 0, 0, u_r^f\right], r = b\end{aligned} \tag{7}$$

3.2. *Thermal boundary conditions*

Isothermal surfaces

$$T = 0 \tag{8}$$

Thermally insulated surfaces

$$T_{,r} = 0$$

3.3. *Electrical boundary conditions*

Electrically shorted (Closed circuits) surfaces

$$D_r = 0$$

Charge free (Open circuits) surfaces

$$V = 0 \tag{9}$$

4. Solutions of the field equation

The Eqs. (6) are coupled partial differential equations of the three displacement components. This system of equations can be uncoupled by eliminating two of the three displacement components through two of the three equations, but this result in partial differential equations of sixth order. To uncouple the Eqs. (6), we follow Paul [31] and assuming the solution of Eqs. (6) as follows:

$$\begin{aligned}u_r(r,\theta,z,t) &= \left(\phi_{,r} + r^{-1}\psi_{,\theta}\right) e^{i(kz+\omega t)} \\ u_\theta(r,\theta,z,t) &= \left(r^{-1}\phi_{,\theta} - \psi_{,r}\right) e^{i(kz+\omega t)} \\ u_z(r,\theta,z,t) &= \left(\frac{i}{a}\right) W e^{i(kz+\omega t)} \\ T(r,\theta,z,t) &= \frac{c_{44}}{\beta_3 a^2} T e^{i(kz+\omega t)} \\ V(r,\theta,z,t) &= iV e^{i(kz+\omega t)} \\ E_r(r,\theta,z,t) &= -E_{,r} e^{i(kz+\omega t)} \\ E_\theta(r,\theta,z,t) &= -r^{-1} E_{,\theta} e^{i(kz+\omega t)} \\ E_z(r,\theta,z,t) &= E_{,z} e^{i(kz+\omega t)}\end{aligned} \tag{10}$$

where $i=\sqrt{-1}$, k is the wave number, ω is the angular frequency, $\phi(r,\theta)$, $W(r,\theta)$, $\psi(r,\theta)$ and $E(r,\theta)$, $T(r,\theta)$ are the displacement potentials and $V(r,\theta)$ is the electric potentials and a is the geometrical parameter of the cylinder.

By introducing the dimensionless quantities such as $x=r/a$, $\zeta=ka$, $\Omega^2=\rho\omega^2a^2/c_{44}$, $\bar{c}_{11}=c_{11}/c_{44}$, $\bar{c}_{13}=c_{13}/c_{44}$, $\bar{c}_{33}=c_{33}/c_{44}$, $\bar{e}_{13}=e_{13}/e_{33}$, $\bar{e}_{15}=e_{15}/e_{33}$, $\bar{\varepsilon}_{11}=\varepsilon_{11}/\varepsilon_{33}$,$\bar{c}_{66}=c_{66}/c_{44}$ and substituting Eq. (10) in Eq. (6), we obtain:

$$\begin{aligned}
&\left(\bar{c}_{11}\nabla^2+\left(\Omega^2-\zeta^2\right)\right)\phi-\zeta\left(1+\bar{c}_{13}\right)W-\zeta\left(\bar{e}_{31}+\bar{e}_{15}\right)V=0\\
&\zeta\left(1+\bar{c}_{13}\right)\nabla^2\phi+\left(\nabla^2+\left(\Omega^2-\zeta^2\bar{c}_{33}\right)\right)W+\left(\bar{e}_{15}\nabla^2-\zeta^2\right)V=0\\
&\overline{\beta}\nabla^2\phi-\zeta W+\left(\overline{d}+i\overline{k}_1\nabla^2-i\overline{k}_3\zeta^2\right)T+\zeta\overline{p}_3V=0\\
&\zeta\left(\bar{e}_{31}+\bar{e}_{15}\right)\nabla^2\phi+\left(\bar{e}_{15}\nabla^2-\zeta^2\right)W+\left(\zeta^2\bar{\varepsilon}_{33}-\bar{\varepsilon}_{11}\nabla^2\right)V=0
\end{aligned}\tag{11}$$

and

$$\left(\bar{c}_{66}\nabla^2+\left(\Omega^2-\zeta^2\right)\right)\psi=0\tag{12}$$

where

$$\nabla^2=\frac{\partial^2}{\partial x^2}+x^{-1}\frac{\partial}{\partial x}+x^{-2}\frac{\partial^2}{\partial\theta^2}$$

The Eq. (11) can be written as the vanishing determinant form

$$\begin{vmatrix} d_{11} & d_{12} & d_{13} & d_{14}\\ d_{21} & d_{22} & d_{23} & d_{24}\\ d_{31} & d_{32} & d_{33} & d_{34}\\ d_{41} & d_{42} & d_{43} & \end{vmatrix}(\phi,W,T,V)=0\tag{13}$$

where:

$$\begin{aligned}
&d_{11}=\bar{c}_{11}\nabla^2+\left(\Omega^2-\zeta^2\right)\quad d_{12}=-\zeta\left(1+\bar{c}_{13}\right)\\
&d_{13}=-\overline{\beta}\quad d_{14}=-\zeta\left(\bar{e}_{31}+\bar{e}_{15}\right)\\
&d_{21}=\zeta\left(1+\bar{c}_{13}\right)\nabla^2\quad d_{22}=\left(\nabla^2+\left(\Omega^2-\zeta^2\bar{c}_{33}\right)\right)\\
&d_{23}=-\zeta\quad d_{24}=\left(\bar{e}_{15}\nabla^2-\zeta^2\right)\\
&d_{31}=\overline{\beta}\nabla^2\quad d_{32}=-\zeta\\
&d_{33}=\left(\overline{d}+i\overline{k}_1\nabla^2-i\overline{k}_3\zeta^2\right)\quad d_{34}=\zeta\overline{p}_3\\
&d_{41}=\zeta\left(\bar{e}_{31}+\bar{e}_{15}\right)\nabla^2\quad d_{42}=\left(\bar{e}_{15}\nabla^2-\zeta^2\right)\\
&d_{43}=\zeta\overline{p}_3\quad d_{44}=\left(\zeta^2\bar{\varepsilon}_{33}-\bar{\varepsilon}_{11}\nabla^2\right)
\end{aligned}$$

Evaluating the determinant given in Eq.(13), we obtain a partial differential equation of the form

$$\left(A\nabla^8+B\nabla^6+C\nabla^4+D\nabla^2+E\right)(\phi,W,T,V)=0\tag{14}$$

where:

$$
\begin{aligned}
&A = -i\overline{k}_1\overline{c}_{11}g_{18}\\
&B = \overline{c}_{11}\left(g_9 - i\overline{k}_1\overline{\varepsilon}_{11}g_2 + \overline{e}_{15}g_{17}\right) + i\overline{k}_1\left(g_1g_{18} - \zeta^2 g_3^2\right) - \overline{\beta}^2 g_{18}\\
&C = \overline{c}_{11}(g_2g_9 + \zeta^2(g_5 + \overline{\varepsilon}_{11} + 2\overline{e}_{15}g_8 - i\overline{k}_1\zeta^2)) + g_1(g_9 - i\overline{k}_1\overline{\varepsilon}_{11}g_2 + \overline{e}_{15}g_{17})\\
&-\overline{\beta}(\overline{\beta}\overline{\varepsilon}_{11}g_2 - \zeta^2(\overline{\beta}\overline{\varepsilon}_{33} - \overline{p}_3g_3 - g_3\overline{e}_{15} + 2\overline{\beta}\overline{e}_{15})) + \zeta^2 g_4(g_4g_{14} + \overline{\beta}\overline{e}_{15} + \zeta g_3g_{15})\\
&-\zeta^2 g_3(i\overline{k}_1\overline{e}_{15}g_4 + \overline{\beta}(\overline{p}_3 + \overline{e}_{15}) - g_3(g_{16} + i\overline{k}_1g_2))\\
&D = \zeta^2\overline{c}_{11}(g_2g_5 - \zeta^2(g_8 - g_7)) + g_1(g_2g_9 + \zeta^2(g_5 + \overline{\varepsilon}_{11} + 2\overline{e}_{15}g_8 - i\overline{k}_1\zeta^2)\\
&+\zeta^2 g_4(g_4(g_{11} + \overline{p}_3\zeta\overline{\varepsilon}_{11}) - \zeta g_3g_{12} - \overline{\beta}\zeta(\zeta + \overline{p}_3^2))\\
&-\overline{\beta}\zeta^2(g_4g_{13} - g_2(\overline{\beta}\overline{\varepsilon}_{33} - \overline{p}_3g_3) - \zeta(g_3 - \overline{\beta}))\\
&-\zeta^2 g_3(g_4g_{11} + g_2(\overline{\beta}\overline{p}_3 - g_3g_{16}) + \zeta^2(g_3 - \overline{\beta}))\\
&E = \zeta^2 g_1g_2g_5 - \zeta^2\left(g_1g_8 - g_1g_7 + g_4^2g_6 + \overline{\beta}g_4g_7 - g_4g_3g_8\right)
\end{aligned}
$$

in which:

$$
\begin{gathered}
g_1 = \Omega^2 - \zeta^2 \quad g_2 = \Omega^2 - \zeta^2\overline{c}_{33} \quad g_3 = \overline{e}_{31} + \overline{e}_{15} \quad g_4 = 1 + \overline{c}_{13}\\
g_5 = \overline{d}\overline{\varepsilon}_3 - i\overline{k}_3\overline{\varepsilon}_{33}\zeta^2 - \overline{p}_3^2 \quad g_6 = \overline{d} + \overline{p}_3\zeta\overline{\varepsilon}_{33} \quad g_7 = \overline{p}_3 - \overline{\varepsilon}_{33} \quad g_8 = \overline{d} - \overline{p}_3 - i\overline{k}_3\zeta^2\\
g_9 = i\overline{k}_1\zeta^2\overline{\varepsilon}_{33} + i\overline{k}_3\overline{\varepsilon}_{11}\zeta^2 - \overline{d}\overline{\varepsilon}_{11} \quad g_{10} = \overline{\varepsilon}_{11} + 2\overline{e}_{15}g_8 - i\overline{k}_1\zeta^2\\
g_{11} = \overline{d}\overline{e}_{15} - i\overline{k}_1\zeta^2 - i\overline{k}_3\zeta^2\overline{e}_{15} \quad g_{12} = \zeta^2\overline{\varepsilon}_{33} + \overline{d}\overline{p}_3 - i\overline{k}_3\overline{p}_3\zeta^2\\
g_{13} = \overline{\varepsilon}_{11} - \overline{p}_3\overline{e}_{15} \quad g_{14} = i\left(\overline{k}_1\overline{e}_{15} + \overline{k}_3\right) \quad g_{15} = \overline{\varepsilon}_{11} - i\overline{p}_3\overline{k}_1 \quad g_{16} = \overline{d}^2 - \zeta^2 i\overline{k}_3\\
g_{17} = i\overline{k}_1\zeta^2 - g_{11} \quad g_{18} = \overline{\varepsilon}_{11} + \overline{e}_{15}^2
\end{gathered}
$$

Factorizing the relation given in Eq. (14) into biquadratic equation for $(\alpha_i a)^2$, $(i = 1, 2, 3, 4)$, the solutions for the symmetric modes are obtained as:

$$
\begin{aligned}
\phi &= \sum_{i=1}^{4}\left[A_iJ_n\left(\alpha_i ax\right) + B_iY_n\left(\alpha_i ax\right)\right]\cos n\theta\\
W &= \sum_{i=1}^{4} a_i\left[A_iJ_n\left(\alpha_i ax\right) + B_iY_n\left(\alpha_i ax\right)\right]\cos n\theta\\
T &= \sum_{i=1}^{4} b_i\left[A_iJ_n\left(\alpha_i ax\right) + B_iY_n\left(\alpha_i ax\right)\right]\cos n\theta\\
V &= \sum_{i=1}^{4} c_i\left[A_iJ_n\left(\alpha_i ax\right) + B_iY_n\left(\alpha_i ax\right)\right]\cos n\theta
\end{aligned}
\tag{15}
$$

Here $(\alpha_i a)^2 > 0, (i = 1, 2, 3, 4)$ are the roots of the algebraic equation

$$
A\left(\alpha a\right)^8 - B\left(\alpha a\right)^6 + C\left(\alpha a\right)^4 - D\left(\alpha a\right)^2 + E = 0 \tag{16}
$$

The solutions corresponding to the root $(\alpha_i a)^2 = 0$ is not considered here, since $J_n(0)$ is zero, except for$n = 0$. The Bessel function J_n is used when the roots

$(\alpha_i a)^2, (i = 1, 2, 3, 4)$are real or complex and the modified Bessel function $I_n$is used when the roots $(\alpha_i a)^2, (i = 1, 2, 3, 4)$are imaginary.

The constants a_i, b_i and c_i defined in the Eq. (14) can be calculated from the equations:

$$\begin{aligned} a_i &= \left(\overline{\beta}\overline{p}_3 - g_3 L\right)/\left(g_4 L + \overline{\beta}\right) \\ b_i &= -\left(g_3\overline{\beta}\left(\alpha_i a\right)^2 + \overline{p}_3\left(g_1 + \overline{c}_{11}\left(\alpha_i a\right)^2\right)\right)\Big/\left(g_4 L + \overline{\beta}\right) \\ c_i &= \left(\left(\alpha_i a\right)^2\left(g_4\overline{\beta} - \overline{c}_{11}\right) - g_1\right)\Big/\left(g_4 L + \overline{\beta}\right) \end{aligned} \tag{17}$$

where

$$L = \left(\overline{d} - i\overline{k}_1\left(\alpha_i a\right)^2 - i\overline{k}_3\zeta^2\right)$$

Solving the Eq. (10), the solution to the anti-symmetric mode is obtained as

$$\psi = A_5\left[J_n\left(\alpha_5 a x\right) + Y_n\left(\alpha_5 a x\right)\right]\sin n\theta \tag{18}$$

where $\left(\alpha_5 a\right)^2 = \Omega^2 - \zeta^2$. If $\left(\alpha_5 a\right)^2 < 0$, the Bessel function J_n is replaced by the modified Bessel function I_n.

5. Equations of motion of the fluid

In cylindrical polar coordinates r, θ and z the acoustic pressure and radial displacement equation of motion for an invicid fluid are of the form Achenbach [32]

$$p^f = -B^f\left(u^f_{r,r} + r^{-1}(u^f_r + u^f_{\theta,\theta}) + u^f_{z,z}\right) \tag{19}$$

and

$$c_f^{-2}u^f_{r,tt} = \Delta_{,r} \tag{20}$$

respectively where B^f, is the adiabatic bulk modulus, ρ^f is the density, $c^f = \sqrt{B^f/\rho^f}$ is the acoustic phase velocity in the fluid, and $\left(u^f_r,\, u^f_\theta,\, u^f_z\right)$ is the displacement vector.

$$\Delta = \left(u^f_{r,r} + r^{-1}(u^f_r + u^f_{\theta,\theta}) + u^f_{z,z}\right) \tag{21}$$

Substituting

$$u^f_r = \phi^f_{,r},\; u^f_\theta = r^{-1}\phi^f_{,\theta}\,\text{and}\,u^f_z = \phi^f_{,z} \tag{22}$$

and seeking the solution of (21) in the form

$$\phi^f(r, \theta, z, t) = \sum_{n=0}^{\infty}\phi^f(r)\cos n\theta e^{i(kz+\omega t)} \tag{23}$$

the oscillating waves propagating in the inner fluid located in the annulus is given by

$$\phi^f = A_5 J_n(\alpha_5 a x) \tag{24}$$

where $(\alpha_5 a)^2 = \Omega^2 \Big/ \overline{\rho}_1^f \overline{B}_1^f - \varsigma^2$, in which $\overline{\rho}_1^f = \rho_1 \big/ \rho^f, \overline{B}_1^f = B_1^f \Big/ c_{44}$. If $(\alpha_5 a)^2 < 0$, the Bessel function J_n in (24) is to be replaced by modified Bessel function I_n. Similarly, for the outer fluid that represents the oscillatory waves propagating away is given as

$$\phi^f = B_5 H_n^{(2)}(\alpha_6 a x) \tag{25}$$

where $(\alpha_6 a)^2 = \Omega^2 \Big/ \overline{\rho}_2^f \overline{B}_2^f - \varsigma^2$, in which $\overline{\rho}_2^f = \rho_2 / \rho^f$, $\overline{B}_2^f = B_2^f \Big/ c_{44}$, $H_n^{(2)}$ is the Hankel function of the second kind. If $(\alpha_6 a)^2 < 0$, then the Hankel function of second kind is to be replaced by K_n, where K_n is the modified Bessel function of the second kind. By substituting Eq. (22) in (19) along with (24) and (25), the acoustic pressure for the inner fluid can be expressed as

$$p_1^f = A_5 \Omega^2 \overline{\rho}_1 J_n(\alpha_5 a x) \cos n\theta e^{i(\varsigma \overline{z} + \Omega T_a)} \tag{26}$$

and for the outer fluid is

$$p_2^f = B_5 \Omega^2 \overline{\rho}_2 H_n^{(2)}(\alpha_6 a x) \cos n\theta e^{i(\varsigma \overline{z} + \Omega T_a)} \tag{27}$$

6. Frequency equations

Substituting the solutions given in the Eqs. (15), (18), (26) and (27) in the boundary conditions given in the Eqs. (7), we obtain a system of eight linear algebraic equations as follows

$$[A]\{X\} = \{0\} \tag{28}$$

where $[A]$ is a 12×12 matrix of unknown wave amplitudes, and $\{X\}$ is an 12×1 column vector of the unknown amplitude coefficients A_1, B_1, A_2, B_2, A_3, B_3, A_4, B_4, and A_5, B_5.... The solution of Eq. (28) is nontrivial when the determinant of the coefficient of the wave amplitudes $\{X\}$ vanishes, that is $|A| = 0$.

The elements in the above determinant is defined as:

$$
\begin{aligned}
&a_{1i} = 2\overline{c}_{66}\left\{n\left(n-1\right)J_n\left(\alpha_i a x\right) + \left(\alpha_i a x\right)J_{n+1}\left(\alpha_i a x\right)\right\}\\
&-x^2\left[\left(\alpha_i a\right)^2\overline{c}_{11} + \zeta\overline{c}_{13}a_i + \zeta b_i + \overline{\beta}c_i\right]J_n\left(\alpha_i a x\right) \quad i = 1,2,3,4\\
&a_{14} = 2\overline{c}_{66}n\left\{\left(n-1\right)J_n\left(\alpha_4 a\right) - \left(\alpha_4 a\right)J_{n+1}\left(\alpha_4 a\right)\right\}\\
&a_{15} = 2\overline{c}_{66}n\left\{\left(n-1\right)Y_n\left(\alpha_4 a\right) - \left(\alpha_4 a\right)Y_{n+1}\left(\alpha_4 a\right)\right\}\\
&a_{1i} = 2\overline{c}_{66}\left\{n\left(n-1\right) - \overline{c}_{11}\left(\alpha_i a\right)^2 - \varsigma\left(\overline{c}_{13}a_i + \overline{e}_{31}b_i\right)\right\}Y_n\left(\alpha_i a\right)\\
&+2\overline{c}_{66}\left(\alpha_i a\right)Y_{n+1}\left(\alpha_i a\right) \quad i = 6,7,8\\
&a_{19} = \overline{\rho}_1\Omega^2 J_n\left(\alpha_5 a\right) \quad a_{10} = \overline{\rho}_2\Omega^2 H_n^{(2)}\left(\alpha_6 a\right) \quad a_{1i} = 0 \quad i = 11,12\\
&a_{2i} = 2n\left\{\left(n-1\right)J_n\left(\alpha_i a\right) + \left(\alpha_i a\right)J_{n+1}\left(\alpha_i a\right)\right\} \quad i = 1,2,3\\
&a_{24} = \left\{\left[\left(\alpha_4 a\right)^2 - 2n\left(n-1\right)\right]J_n\left(\alpha_4 a\right) - 2\left(\alpha_4 a\right)J_{n+1}\left(\alpha_4 a\right)\right\}\\
&a_{25} = \left\{\left[\left(\alpha_4 a\right)^2 - 2n\left(n-1\right)\right]Y_n\left(\alpha_4 a\right) - 2\left(\alpha_4 a\right)Y_{n+1}\left(\alpha_4 a\right)\right\}\\
&a_{2i} = 2n\left\{\left(n-1\right)Y_n\left(\alpha_i a\right) + \left(\alpha_i a\right)Y_{n+1}\left(\alpha_i a\right)\right\} \quad i = 6,7,8\\
&a_{2i} = 0,\ i = 9,10,11,12\\
&a_{3i} = \left(\left(\varsigma + a_i\right) + \overline{e}_{15}b_i\right)\left\{nJ_n\left(\alpha_i a\right) - \left(\alpha_i a\right)J_{n+1}\left(\alpha_i a\right)\right\} \quad i = 1,2,3\\
&a_{34} = n\varsigma J_n\left(\alpha_4 a\right) \quad a_{35} = n\varsigma Y_n\left(\alpha_4 a\right)\\
&a_{3i} = \left(\left(\varsigma + a_i\right) + \overline{e}_{15}b_i\right)\left\{nJ_n\left(\alpha_i a\right) - \left(\alpha_i a\right)J_{n+1}\left(\alpha_i a\right)\right\} \quad i = 6,7,8\\
&a_{3i} = 0,\ i = 9,10,11,12\\
&a_{4i} = b_i J_n\left(\alpha_i a\right) \quad i = 1,2,3 \quad a_{44} = 0 \quad a_{45} = 0\\
&a_{4i} = b_i Y_n\left(\alpha_i a\right) \quad i = 6,7,8 \quad a_{4i} = 0 \quad i = 9,10,11,12\\
&a_{5i} = \left\{nJ_n\left(\alpha_i a\right) - \left(\alpha_i a\right)J_{n+1}\left(\alpha_i a\right)\right\} \quad i = 1,2,3 \quad a_{54} = nJ_n\left(\alpha_4 a\right)\\
&a_{55} = nY_n\left(\alpha_4 a\right) \quad a_{5i} = \left\{nY_n\left(\alpha_i a\right) - \left(\alpha_i a\right)Y_{n+1}\left(\alpha_i a\right)\right\} \quad i = 6,7,8\\
&a_{59} = \Omega^2\overline{\rho}_1\left\{nJ_n\left(\alpha_5 a\right) - \left(\alpha_5 a\right)J_{n+1}\left(\alpha_5 a\right)\right\}\\
&a_{510} = \Omega^2\overline{\rho}_2\left\{nH_n^{(2)}\left(\alpha_6 a\right) - \left(\alpha_6 a\right)H_{n+1}^{(2)}\left(\alpha_6 a\right)\right\} \quad a_{5i} = 0 \quad i = 11,12\\
&a_{6i} = c_i\left\{nJ_n\left(\alpha_i a x\right) - \left(\alpha_i a x\right)J_{n+1}\left(\alpha_i a x\right)\right\} \quad i = 1,2,3 a_{64} = nJ_n\left(\alpha_4 a\right)\\
&a_{65} = nY_n\left(\alpha_4 a\right)\\
&a_{6i} = \left(\left(\varsigma + a_i\right) + \overline{e}_{15}b_i\right)\left\{nJ_n\left(\alpha_i a\right) - \left(\alpha_i a\right)J_{n+1}\left(\alpha_i a\right)\right\} \quad i = 6,7,8\\
&a_{6i} = 0,\ i = 9,10,11,12
\end{aligned}
$$

The complex secular Eq. (28) contains complete information regarding wave number, phase velocity and attenuation coefficient and other propagation characteristics of the considered surface waves. In order to solve this equation we take

$$c^{-1} = v^{-1} + i\omega^{-1}q \tag{29}$$

where $\zeta = R + iq$, $R = \frac{\omega}{v}$ and R, q are real numbers. Here it may be noted that v and q respectively represent the phase velocity and attenuation coefficient of the waves. Upon using the representation (29) in Eq. (28) and various relevant relations, the complex roots $\alpha_i (i = 1,2,3,4)$ of the Eq. (15) can be computed with the help of

Secant method. The characteristics roots $\alpha_i (i = 1, 2, 3, 4)$ are further used to solve the Eq. (28) to obtain phase velocity(v) and attenuation coefficient (q) by using the functional iteration numerical technique as given below.

The Eq.(28) is of the form $F(C) = 0$ which upon using representation (29) leads to a system of two real equations $f(v, q) = 0$ and $g(v, q) = 0$. In order to apply functional iteration method, we write $v = f^*(v, q)$ and $q = g^*(v, q)$, where the functions f^* and g^* are selected in such a way that they satisfies the conditions

$$\left|\frac{\partial f^*}{\partial v}\right| + \left|\frac{\partial g^*}{\partial q}\right| < 1 \left|\frac{\partial g^*}{\partial v}\right| + \left|\frac{\partial f^*}{\partial q}\right| < 1 \tag{30}$$

For all v, q in the neighborhood of the roots. If (v_0, q_0) be the initial approximation of the root, then we construct a successive approximation according to the formulae:

$$\begin{array}{ll} v_1 = f^*(v_0, q_0) & q_1 = g^*(v_1, q_0) \\ v_2 = f^*(v_1, q_1) & q_2 = g^*(v_2, q_1) \\ v_3 = f^*(v_2, q_2) & q_3 = g^*(v_3, q_2) \\ \ldots\ldots\ldots\ldots\ldots\ldots & \ldots\ldots\ldots\ldots\ldots\ldots \\ v_n = f^*(v_n, q_n) & q_n = g^*(v_{n+1}, q_n) \end{array} \tag{31}$$

The sequence $\{v_n, q_n\}$ of approximation to the root will converge to the actual value (v_0, q_0) of the root provided(v_0, q_0)lie in the neighborhood of the actual root. For the initial value $c = c_0 = (v_0, q_0)$, the roots $\alpha_i (i = 1, 2, 3, 4)$ are computed from the Eq. (15) by using Secant method for each value of the wave number ζ, for assigned frequency. The values of $\alpha_i (i = 1, 2, 3, 4)$ so obtained are then used in the Eq.(28) to obtained the current values of v and q each time which are further used to generate the sequence (30). This process is terminated as and when the condition $|v_{n+1} - v_n| < \varepsilon$, ε being arbitrary small number to be selected at random to achieve the accuracy level, is satisfied. The procedure is continually repeated for different values of the wave number (ζ) to obtain the corresponding values of the phase velocity (v) and attenuation coefficient (q).

6.1. *Particular case*

The frequency equation for a piezoelectric solid circular cylinder is obtained discarding the inner and outer fluid medium, thermal field in the corresponding equations and solutions along with the outer boundary conditions, and substitute in the solution and frequency equations Y_n and Y_{n+1} is equal to zero. The frequency equations obtained in this method matches well with the frequency equations of Paul and Raju [31] which shows the exactness of this method.

6.2. *Specific loss*

The internal energy of a material is defined by specific loss. The specific loss is the ratio of the amount of energy (ΔE) dissipated in a specimen through a stress cycle to the elastic energy (E) stored in that specimen at a maximum strain. According to Kolsky [33], specific loss $(\Delta E/E)$ is equal to 4π times the absolute value of the imaginary part of ζ to the real part of ζ, therefore we have

$$S.L = |\Delta E/E| = 4\pi \left|Im\left(\zeta\right)/Re\left(\zeta\right)\right| = |v_q/\omega| \tag{32}$$

The real and imaginary parts of the wave number is obtained from the relation $\zeta = R + iq$, where $R = \omega/\nu$ and the wave speed (v) and the attenuation coefficient (q) are real numbers.

6.3. *Thermo mechanical coupling*

The coupling effect between thermal and elasticity in a thermo elastic material provides a mechanism for sensing thermo mechanical disturbance from measurements of induced magnetic potentials, and for altering structural responses through applied magnetic fields in the design of sensors and surface acoustic damping wave filters. Thermo mechanical coupling factor is defined as

$$\kappa^2 = \left| \frac{V_1 - V_2}{V_2} \right| \tag{33}$$

where V_1 is the phase velocity of the wave under thermally insulated boundary and V_2phase velocity of the wave under isothermal boundary.

7. Numerical examples and discussion

The frequency equation given in Eq. (28) is transcendental in nature with unknown frequency and wave number. The solutions of the frequency equation are obtained numerically by fixing the non–dimensional wave number. The material properties of PZT-5A and PZT-4A are taken from Berlincourt et al [34] are used for the numerical calculation is given below:

Example 1: Consider the fluid filled and immersed piezo-thermo elastic hollow cylinder with the material properties of PZT-5A

$$\begin{aligned}
&c_{11} = 13.9 \times 10^{10} Nm^{-2} \quad c_{12} = 7.78 \times 10^{10} Nm^{-2} \quad c_{13} = 7.43 \times 10^{10} Nm^{-2} \\
&c_{33} = 11.3 \times 10^{10} Nm^{-2} \quad c_{44} = 2.56 \times 10^{10} Nm^{-2} \quad c_{66} = 3.06 \times 10^{10} Nm^{-2} \\
&\beta_1 = 1.52 \times 10^{6} NK^{-1}m^{-2} \quad \beta_3 = 1.53 \times 10^{6} NK^{-1}m^{-2} \\
&T_0 = 298K \quad c_v = 420 \quad Jkg^{-1}K^{-1} \quad p_3 = -452 \times 10^{-6} CK^{-1}m^{-2} \\
&K_1 = K_3 = 1.5 \quad Wm^{-1}K^{-1} \quad e_{13} = -6.98 Cm^{-2} \quad e_{33} = 13.8 Cm^{-2} \\
&e_{51} = 13.4 Cm^{-2} \quad \varepsilon_{11} = 60.0 \times 10^{-10} C^2 N^{-1} m^{-2} \\
&\varepsilon_{33} = 54.7 \times 10^{-10} C^2 N^{-1} m^{-2} \quad \rho = 7500 Kgm^{-2}
\end{aligned}$$

and for fluid the density $\rho^f = 1000$ Kgm^{-3}, phase velocity $c = 1500$ m/s^{-1} and used for the numerical calculations.

In Tabs 2 and 3 the absolute, real and imaginary values the non–dimensional wave number are given against dimensionless frequency for the two cases of electrically shorted (Closed circuits) and charge free (Open circuits) boundary conditions. The Tabs 2 and 3 clarifies that as the dimensionless frequency increases the non–dimensional wave number also increases in both the electrical boundary conditions. The computed dimensionless frequency, phase velocity, attenuation, thermo elastic coupling and specific loss are plotted in the form of dispersion curves in Fig. 2–11.

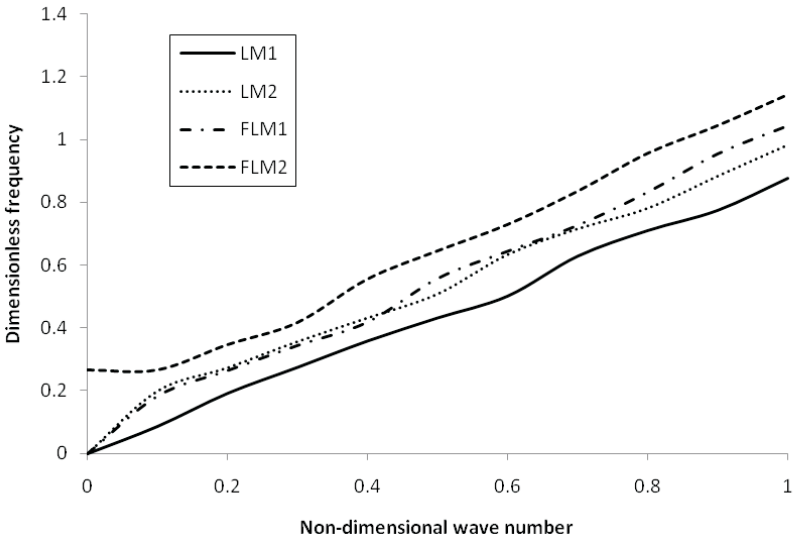

Figure 2 Dimensionless frequency versus non–dimensional wave number |for isothermal modes of fluid–loaded piezo–thermo elastic cylinder immersed in fluid

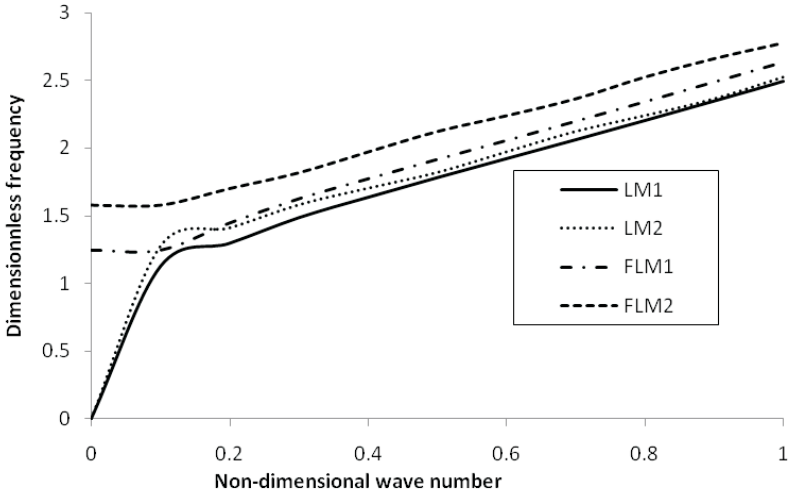

Figure 3 Dimensionless frequency versus non–dimensional wave number for thermally insulated modes of fluid–loaded piezo–thermo elastic cylinder immersed in fluid

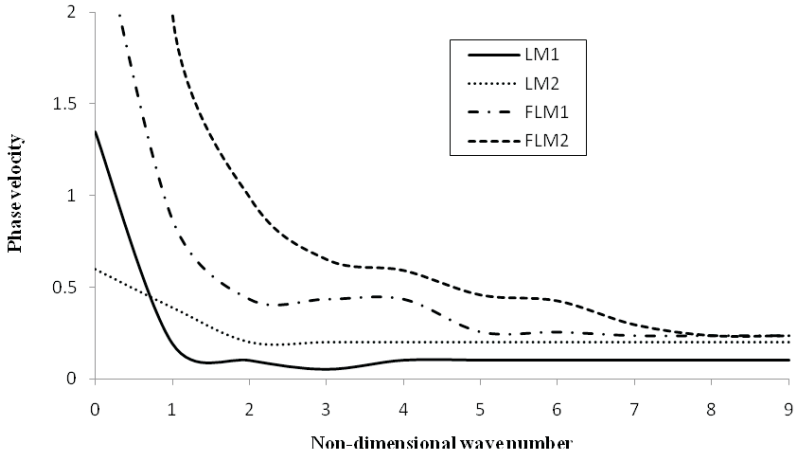

Figure 4 Phase velocity versus non–dimensional wave number for isothermal modes of fluid–loaded piezo–thermo elastic cylinder immersed in fluid

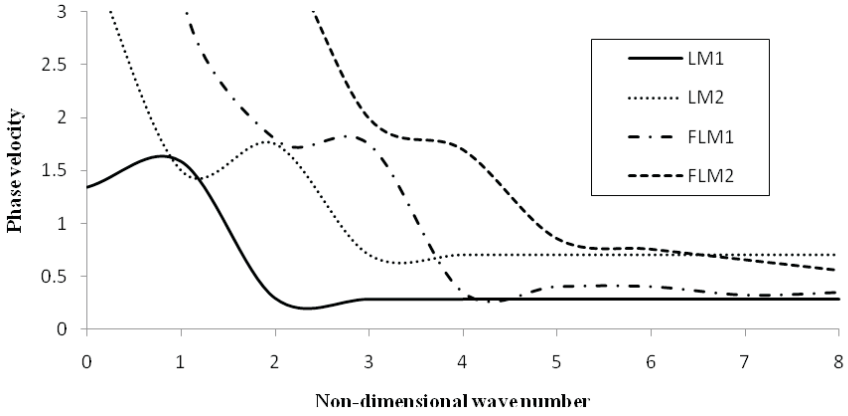

Figure 5 Phase velocity versus non–dimensional wave number for thermally insulated modes of fluid–loaded piezo–thermo elastic cylinder immersed in fluid

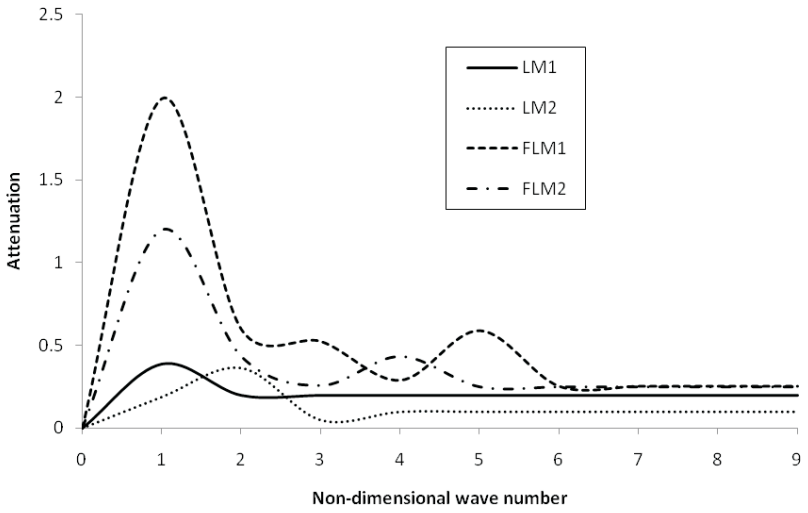

Figure 6 Attenuation versus non–dimensional wave number for isothermal modes of fluid-loaded piezo–thermo elastic cylinder immersed in fluid

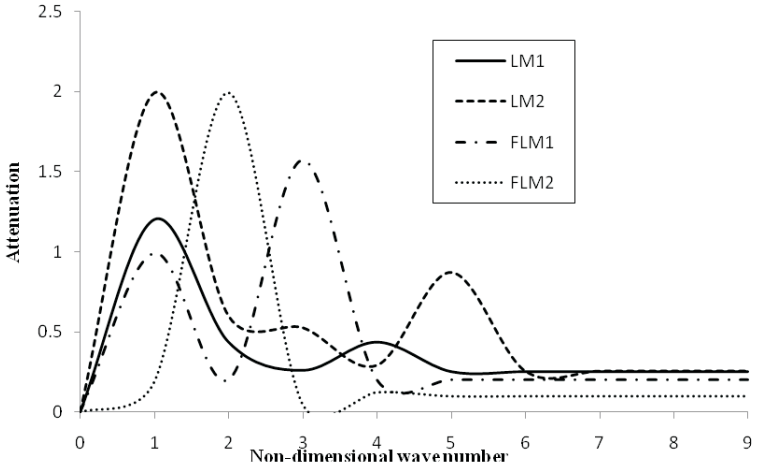

Figure 7 Attenuation versus non-dimensional wave number for thermally insulated modes of fluid-loaded piezo–thermo elastic cylinder immersed in fluid

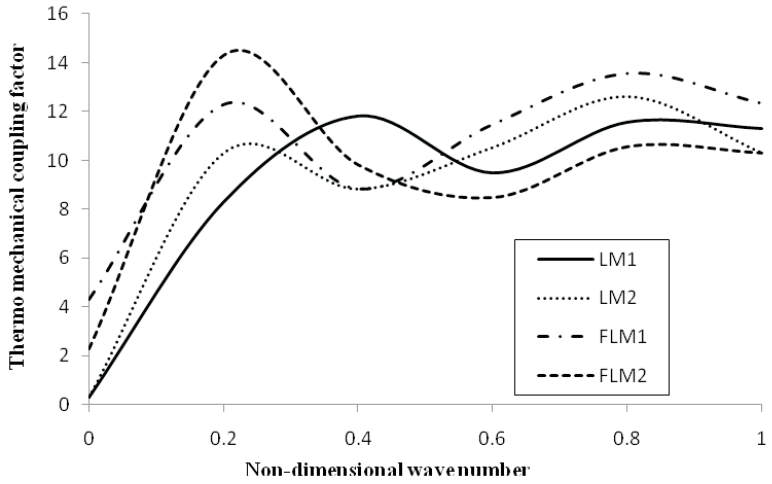

Figure 8 Thermo mechanical coupling factor versus non–dimensional wave number for isothermal modes of fluid-loaded piezo–thermo elastic cylinder immersed in fluid

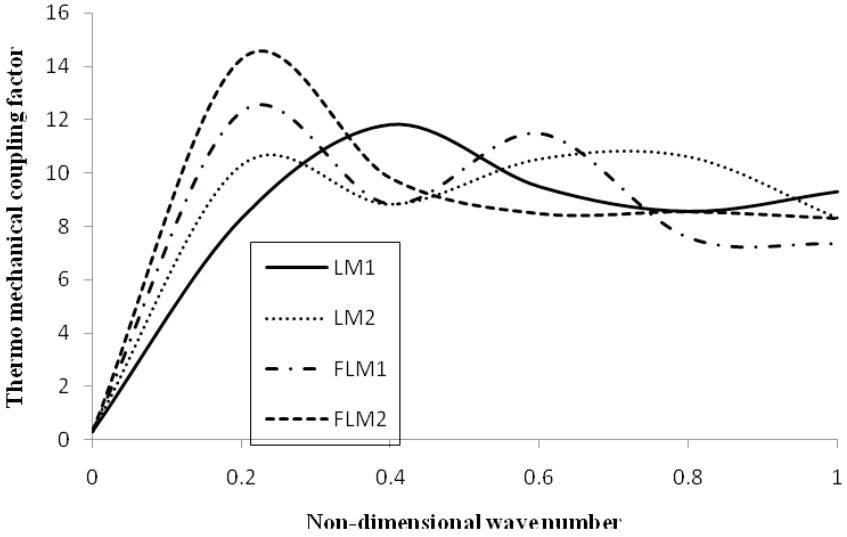

Figure 9 Thermo mechanical coupling factor versus non–dimensional wave number for thermally insulated modes of fluid-loaded piezo–thermo elastic cylinder immersed in fluid

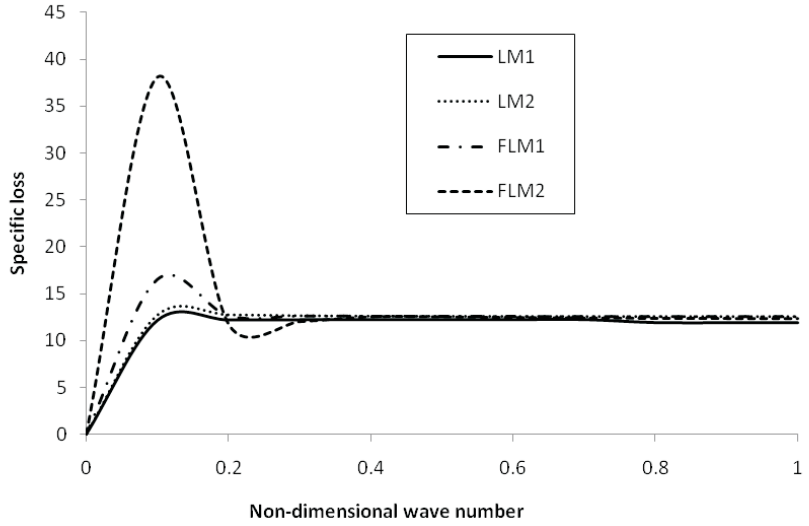

Figure 10 Specific loss versus non–dimensional wave number for isothermal modes of fluid-loaded piezo–thermo elastic cylinder immersed in fluid

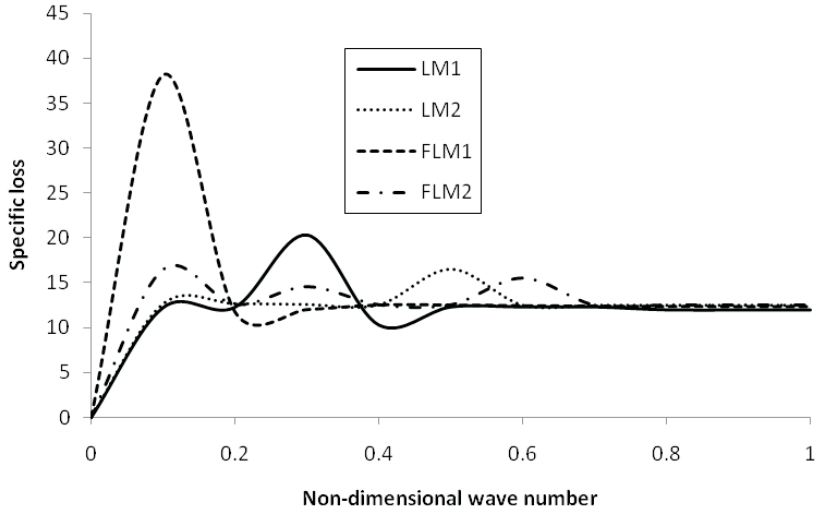

Figure 11 Specific loss versus non–dimensional wave number for thermally insulated modes of fluid–loaded piezo–thermo elastic cylinder immersed in fluid

Example 2: Consider the transversely isotropic piezo–electric circular cylinder with the material properties of PZT-4A:

$$c_{11} = 13.9 \times 10^{10} Nm^{-2} \quad c_{12} = 7.78 \times 10^{10} Nm^{-2} \quad c_{13} = 7.43 \times 10^{10} Nm^{-2}$$
$$c_{33} = 11.5 \times 10^{10} Nm^{-2} \quad c_{44} = 2.56 \times 10^{10} Nm^{-2} \quad c_{66} = 3.06 \times 10^{10} Nm^{-2}$$
$$e_{31} = -5.2 Cm^{-2} \quad e_{33} = 15.1 Cm^{-2} \quad e_{15} = 12.7 Cm^{-2}$$
$$\varepsilon_{11} = 6.46 \times 10^{-9} C^2 N^{-1} m^{-2} \quad \varepsilon_{33} = 5.62 \times 10^{-9} C^2 N^{-1} m^{-2}$$

The frequency equation for a piezoelectric circular cylinder of infinite length without fluid medium is obtained by omitting the inner, outer fluid medium and thermo coupling and substituting Y_n and Y_{n+1} equal to zero in the solutions and frequency equation, thus we obtain the frequency equation for a piezoelectric solid circular cylinder. This frequency equation is compared with the frequency equations of Paul and Raju [31], which matches well with the frequency equations of the author. The non-dimensional frequencies are obtained using secant method for $0 < \varsigma \leq 0.1$ for the material PZT-4 and this frequencies are matches well with the non–dimensional frequencies obtained by Paul and Raju [31] is given in Table 1 which shows the exactness of the author's method. From the Table 1, it is observed that, the non–dimensional frequencies Ω are increases with respect to its wave number ς, also this analysis clearly displays the structure of the frequency spectrum near the cut of frequencies.

Table 1 Comparison of longitudinal mode of frequencies Ω of author with Paul and Raju [31] for an infinite solid cylinder of PZT-4

ς	n = 0		n = 1		n = 2	
	Author	Paul and Raju	Author	Paul and Raju	Author	Paul and Raju
0.01	4.6654	4.6655	1.8911	1.8911	3.1815	3.1816
	8.5421	8.5424	6.4147	6.4143	8.0351	8.0351
	12.3876	12.3875	10.3462	10.3469	12.0568	12.0561
	16.2235	16.2234	14.2201	14.2195	15.9751	15.9750
0.04	4.6667	4.6641	1.8913	1.8923	3.1824	3.1825
	8.5423	8.5425	6.4145	6.4142	8.0351	8.0351
	12.3844	12.3873	10.3471	10.3479	12.0564	12.0563
	16.2237	16.2234	14.2195	14.2195	15.9754	15.9751
0.1	4.6566	4.6566	1.8991	1.8992	3.1870	3.1869
	8.5426	8.5427	6.4135	6.4137	8.0351	8.0348
	12.3859	12.3858	10.3472	10.3475	12.0573	12.0578
	16.2234	16.2235	14.2193	14.2195	15.9756	15.9757

Table 2 Absolute value of the non–dimensional wave number for the two cases of electrical boundaries with dimensionless frequency

Ω	Longitudinal mode		Flexural mode	
	Open	Closed	Open	Closed
0.1	1.2897	1.3595	1.5565	1.5572
0.3	1.6443	1.5726	1.8401	1.8402
0.5	1.8563	1.7824	2.1209	2.1236
0.7	2.0820	1.9813	2.4042	2.4040
1.0	2.4248	2.2932	2.8301	2.8311

Table 3 Real and imaginary value of the non–dimensional wave number for the two cases of electrical boundaries with dimensionless frequency

Ω	Longitudinal mode				Flexural mode			
	Open		Closed		Open		Closed	
	Real (ζ)	Imag (ζ)	Real (ζ)	Imag (ζ)	Real (ζ)	Imag (ζ)	Real (ζ)	Imag (ζ)
0.1	0.9108	0.9030	0.9416	0.9301	1.1013	1.1009	1.1011	1.1011
0.3	1.1612	1.1542	1.1183	1.1138	1.3027	1.3016	1.3013	1.3011
0.5	1.3120	1.2132	1.2592	1.2115	1.4992	1.5002	1.5009	1.5022
0.7	1.4727	1.4717	1.4014	1.4006	1.6988	1.7012	1.7001	1.6997
1.0	1.7171	1.7020	1.6246	1.6184	2.0024	1.9999	2.0020	2.0018

7.1. *Dispersion curves*

In this problem, there are two kinds of basic independent modes of wave propagation have been considered, namely, the longitudinal and flexural modes. By choosing respectively n = 0 and n = 1, we can obtain the non–dimensional frequencies of longitudinal and flexural modes of vibrations. The notation used in the figures, namely LM and FLM respectively denote the longitudinal mode and flexural mode. The 1 refers the first mode, 2 refers the second mode and so on.

The dispersion curves are drawn for dimensionless frequency Ω versus the non–dimensionl wave number $|\varsigma|$ for isothermal and thermally insulated boundaries of piezo–thermo elatic fluid–loaded hollow cylinder immersed in fluid are respectively shown in Figs. 2 and 3. From the Fig. 2, it is observed that the non–dimensional frequency of the piezo-thermoelatic hollow cylinder shows almost linear variation with respect to wave number for the isothermal boundary. But in Fig. 3, some non–linearity nature is observed between $0 \leq |\varsigma| \leq 0.2$ due to the damping effect of thermal insulation and surrounding fluid medium. From Figs. 2 and 3, the radiation of energy is higher in flexural mode compared with longitudinal modes of vibration.

The variation of the phase velocity(v) with respect to the non–dimensional wave number $|\varsigma|$of the piezo-thermo elastic hollow cylinder with the isothermal and thermally insulated boundaries is shown in Figs. 4 and 5, respectively. From these curves it is clear that the phase velocity curves are strong and sensitive only at

the small values of wave number in the range $0 \leq |\varsigma| \leq 4$ in Figs. 3 and 4, but for higher values of wave number, these become linear and non–dispersive for both the boundaries of thermally insulated and isothermal. This type of phenomenon explains the concept that, as the wave goes to the deeper in the medium (Higher wave number) the coupling effect of various interacting fields increases which leads to lower phase velocity. But there is a small oscillation of cut of frequency in Fig. 5 which might happen because of the radiation of the sound energy in to the fluid produces damping in the system.

The dispersion of attenuation coefficient (q) with respect to the non–dimensional wave number $|\varsigma|$ of the fluid filled and immersed piezo-thermo elastic hollow cylinder is discussed for the two cases of isothermal and thermally insulated boundaries in Fig. 6 and 7. The amplitude of displacement of the attenuation coefficient increases monotonically to attain maximum value in $0 \leq |\varsigma| \leq 2$ and slashes down to became asymptotically linear in the remaining range of the wave number in Fig. 6. The variation of attenuation coefficient for longitudinal and flexural modes of vibration is oscillating in the starting range of wave number as shown in Fig. 7 for thermally insulated boundary. From Fig. 6 and 7, it is clear that the attenuation profiles exhibits high oscillating nature in the small wave number range since, the energy radiation is more sensitive in the surface areas. The cross over points in the vibrational modes indicates the energy transfer between the solid and fluid medium.

In Fig. 8 and 9 the effect of the specific loss ($S.L$) factor for isothermal and thermally insulated boundaries are discussed non–dimensional wave number $|\varsigma|$. The magnitude of the energy dissipation (specific loss) factor is attaining maximum value at $0 \leq |\varsigma| \leq 0.2$ for the fluid filled and immersed piezo–thermo elastic hollow cylinder in Fig. 8. But for thermally insulated mode, the specific loss is getting oscillating trend up to $|\varsigma| \leq 0.7$. On comparison of Fig. 8 and 9 it is clear that the specific loss factor is quiet high when the wave penetrates deep in to the medium.

Fig. 10 and 11 represents the variation of the thermo mechanical coupling $\left(\kappa^2\right)$ factor with non–dimensional wave number $|\varsigma|$ for isothermal and thermally insulated fluid filled and immersed piezo–thermo elastic hollow cylinder. The magnitude of the coupling factor increasing monotonically at small wave number and become steady for higher wave number for both isothermal and thermally insulated boundaries. The effect of thermo mechanical coupling factor is high at lower wave number because of the dissipation of energy is more sensitive on the surface of the hollow cylinder.

8. Conclusions

The dispersion equation of a transversely isotropic piezo–thermo elastic cylinder that is fluid-filled and immersed in fluid is developed from the three-dimensional equations of elasticity and the assumptions of perfect–slip boundary conditions at the solid fluid interfaces. The frequency equations are obtained for longitudinal and flexural modes of vibration and are studied numerically for the material PZT-5A, which is fluid–filled and immersed in fluid. The computed dimensionless frequency, phase velocity, attenuation, thermo mechanical coupling factor and specific loss are plotted in the form of dispersion curves for the material PZT-5A. Discarding the fluid medium and thermo coupling, a comparison is made between the frequency

response of a piezoelectric solid circular cylinder with the existing literature results of Paul and Raju [31], which shows very good agreement. The obtained results are valuable for the analysis of design of piezo thermo elastic transducer and sensors using composite materials and can be utilized in electronics and navigation applications.

References

[1] **Meeker, T. R. and Meitzler, A. H.**: Guided wave propagation in elonged cylinders and plates, in: Mason, W.P. (Ed.), *Physical Acoustics, Academic*, New York, **1964**.

[2] **Mirsky, I.:** Wave propagation in transversely isotropic circular cylinders, Part I: Theory, Part II: Numerical results, *Journal of Acoustical Society of America*, 37, 1016–1026, **1965**.

[3] **Morse, R. W.**: Compressional waves along an anisotropic circular cylinder having hexagonal symmetry, *Journal of Acoustical Society of America*, 26, 1018–1021, **1954**.

[4] **Tiersten, H. F.**: Linear piezoelectric plate vibrations, *Plenum*, New York, **1969**.

[5] **Parton, V.Z. and Kudryavtsev, B.A.:** Electromagnetoelasticity. Gordon and Breach, New York,**1988**.

[6] **Shul'ga, N. A.**: Propagation of harmonic waves in anisotropic piezoelectric cylinders. Homogeneous piezoceramic wave guides, *International Journal of Applied Mechanics*, 38(12), 933–953, **2002**.

[7] **Rajapakse, R. K. N. D. and Zhou, Y.**: Stress analysis of piezo-ceramic cylinders, *Smart Material and Structures*, 6, 169–177, **1997**.

[8] **Wang, Q.**: Axi–symmetric wave propagation in cylinder coated with a piezoelectric layer, *International journal of Solids and Structures*, 39, 3023–3037, **2002**.

[9] **Ebenezer, D. D. and Ramesh, R.**: Analysis of axially polarized piezoelectric cylinders with arbitrary boundary conditions on the flat surfaces, *Journal of Acoustical Society of America*, 113(4), 1900–1908, **2003**.

[10] **Berg, M. and Hagedorn, P. S.**: Gutschmidt, on the dynamics of piezoelectric cylindrical shell, *Journal of Sound and Vibration*, 274, 91–109, **2004**.

[11] **Botta, F. and Cerri, G.**: Wave propagation in Reissner–Mindlin piezoelectric coupled cylinder with non–constant electric field through the thickness, *International Journal of Solids and Structures*, 44, 6201–6219, **2007**.

[12] **Kim, J. O. and Lee, J. G.**: Dynamic characteristics of piezoelectric cylindrical transducers with radial polarization, *Journal of Sound and Vibration*, 300, 241–249, **2007**.

[13] **Mindlin, R. D.**: On the equations of motion of piezoelectric crystals, in: Problems of continuum mechanics, *SIAM*, Philadelphia, 70, 282–290, **1961**.

[14] **Mindlin, R. D.**: Equation of high frequency vibrations of thermo-piezoelectric, crystal plates, Interactions in Elastic Solids, *Springer*, Wien, **1979**.

[15] **Nowacki, W.**: Foundations of linear piezoelectricity, in H. Parkus (Ed.), *Electromagnetic Interactions in Elastic Solids*, *Springer*, Wien, (1),**1979**.

[16] **Nowacki, W.**: Some general theorems of thermo-piezoelectricity, *Journal of Thermal Stresses*, 171–182, **1978**.

[17] **Chandrasekhariah, D. S.**: A temperature rate dependent theory of piezoelectricity, *Journal of thermal stresses*, 7, 293–306, **1984**.

[18] **Chandrasekhariah, D. S.**: A generalized linear thermoelasticity theory of piezoelectric media, *Acta Mechanica*, 71, 39–49, **1988**.

[19] **Yang, J. S. and Batra, R. C.**: Free vibrations of a linear thermo–piezoelectric body, *Journal of thermal stresses*, 18, 247–262, **1995**.

[20] **Sharma, J. N. and Pal, M.**: Propagation of Lamb waves in a transversely isotropic piezothermoelastic plate, *Journal of Sound and Vibration*, 270, 587–610, **2004**.

[21] **Sharma, J. N., Pal, M and Chand, D.**: Three dimensional vibrational analysis of a piezothermoelastic cylindrical panel, *International Journal of Engineering Science*, 42, 1655–1673, **2004**.

[22] **Ponnusamy, P.**: Wave propagation in a generalized thermo elastic solid cylinder of arbitrary cross–section, *International Journal of Solids and Structures*, 44, 5336–5348, **2007**.

[23] **Ponnusamy, P. and Selvamani, R.**: Dispersion analysis of generalized magneto–thermoelastic waves in a transversely isotropic cylindrical panel, *Journal of Thermal Stresses*, 35, 1119–1142, **2012**.

[24] **Sinha, K., Plona, J., Kostek, S and Chang, S.**: Axisymmetric wave propagation in a fluid–loaded cylindrical shell I: Theory; II Theory versus experiment, *Journal of Acoustical Society of America*, 92, 1132–1155, **1992**.

[25] **Berliner, J. and Solecki, R.**: Wave propagation in a fluid-loaded, transversely isotropic cylinders, Part I Analytical Formulation; Part II Numerical results, *Journal of Acoustical Society of America*, 99, 1841–1853, **1996**.

[26] **Selvamani, R. and Ponnusamy, P.**: Wave propagation in a generalized thermo elastic plate immersed in fluid, *Structural Engineering and Mechanics*, 46(6), 827–842, **2013**.

[27] **Selvamani, R. and Ponnusamy, P.**: Dynamic response of a solid bar of cardioidal cross–sections immersed in an inviscid fluid, *Applied Mathematics and Information Sciences*, 8(6), 2909–2919, **2014**.

[28] **Dayal, V.**: Longitudinal waves in homogeneous anisotropic cylindrical bars immersed in fluid, *Journal of Acoustical Society of America*, 93, 1249–1255, **1993**.

[29] **Nagy, B.**: Longitudinal guided wave propagation in a transversely isotropic rod immersed in fluid, *Journal of Acoustical Society of America*, 98(1), 454–457,**1995**.

[30] **Paul, H.S. and Raju, D.P.:** Asymptotic analysis of the modes of wave propagation in a piezoelectric solid cylinder, *Journal of Acoustical Society of America*, 71(2), 255–263, **1982**.

[31] **Paul, H.S.:** Vibrations of circular cylindrical shells of piezo-electric silver iodide crystals, *Journal of Acoustical Society of America*, 40(5), 1077–1080, **1966**.

[32] **Achenbach, J. D.**: Wave motion in elastic solids, *North-Holland: Amsterdam*, **1973**.

[33] **Kolsky, H.**: Stress waves in solids, *New York, London: Dover Press*, **1935**.

[34] **Berlincourt, D. A., Curran D. R and Jaffe, H.**: Piezoelectric and piezomagnetic materials and their function in transducers, New York and London, *Academic Press*, **1964**.